3D RINGLET: Spherical Shells Trajectory for Self-Navigated 3D MRI

Y. Shu[1], A. M. Elliott[1], S. J. Riederer[1], M. A. Bernstein[1]

[1]Department of Radiology, Mayo College of Medicine, Rochester, Minnesota, United States

Introduction:

Patient motion remains a substantial problem for many 3D MRI applications. Current solutions to suppress motion artifacts include physical restraint, or the use of navigator echoes. The former may cause patient discomfort, while the latter requires additional acquisition time. We describe a 3D data acquisition method that is self-navigated, i.e. the motion tracking information is embedded in the desired image data itself. Redundant acquisition of k-space data points is not required, although three point-source markers are. With a new interleaved shell trajectory, each time bin of the acquisition is reconstructed into a 3D tracking image in which the point sources display a characteristic bull's-eye pattern. Thus the proposed method is a generalization of the RINGLET method [1]. Rigid body motion can be measured and corrected retrospectively in all six degrees of freedom.

Theory and Methods:

The shell trajectory: The spherical shell trajectory [2] samples 3D k-space with spirals (i.e., tapered helices) along the surfaces of concentric spheres, as shown in Figure 1. An initial phase encoding blip moves the trajectory to the starting point on the spherical shell. Interleaved spirals are then traced on the spherical shell surfaces. The scan starts from the shell with smallest radius, i.e., $0.5\Delta k$, although the center-most volume can alternatively be acquired with Cartesian sampling to reduce sensitivity to off-resonant effects. Shells are acquired with increasing radius until the prescribed maximum of k-space radius is reached. The parametric equations describing spherical trajectories have been described for RF excitation in [3], and spherical shell navigators are described in [4]. To satisfy the Nyquist sampling criterion, the number of helical interleaves can vary for each shell, with more interleaves generally required at larger radii. Due to gradient slew rate limitations, the helical spirals are not able to reach the polar ice cap of the shells. To cover the polar ice caps, two additional spiral interleaves are used. Raw data were reconstructed with a 3D gridding algorithm [5] followed by inverse Fourier Transform.

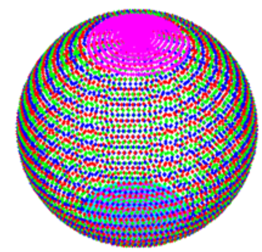

Fig. 1 k-space sampling with shell trajectory. Different colors represent multiple interleaves of helical spirals. The polar ice cap parts are sampled by two additional spirals.

3D motion detection: With this trajectory, a set of spherical shells in k-space is sampled during each time interval in the acquisition. Patient motion during a time interval corrupts the corresponding shells of data. The raw data set is subdivided into consecutive spherical shells regions, which are then reconstructed to yield a series of 3D tracking images. In each set of tracking images, a point object displays a radially symmetric bull's-eye pattern irrespective of k-space radius. The true location of the point object is located in the center of the bulls-eye pattern. The motion of the imaged object can be tracked using three point-markers. For clinical situations, the markers can be embedded in a pair of headphones for comfort. By registering the marker positions in consecutive shells, the motion history of the object can be established and corrected.

3D motion correction: Rigid body motion of the object can be modeled with a combination of rotation and translation. Translation in image space can be corrected by linear phase correction in k-space. Rotation of the object corresponds to a corresponding rotation in k-space. Off-center rotations are mathematically equivalent to an on-center rotation and translations of the coordinates.

Results:

The shells trajectory: A prototype shell trajectory was implemented on a GE 1.5T Signa scanner. To demonstrate feasibility, a matrix of 88×88×88 pixels over a 25.6×25.6×25.6 cm^3 field of view was acquired with a brain phantom. The readout duration was 7.2 ms with a ±62.5 kHz bandwidth. A total of 775 TR intervals were required for the acquisition. The resultant scan time was 60% lower than a conventional 3DFT trajectory with equivalent field of view and resolution, although some of the scan time advantage can be traded for shorter helical readouts, which will require more interleaves. Each readout sampled 900 complex data points.

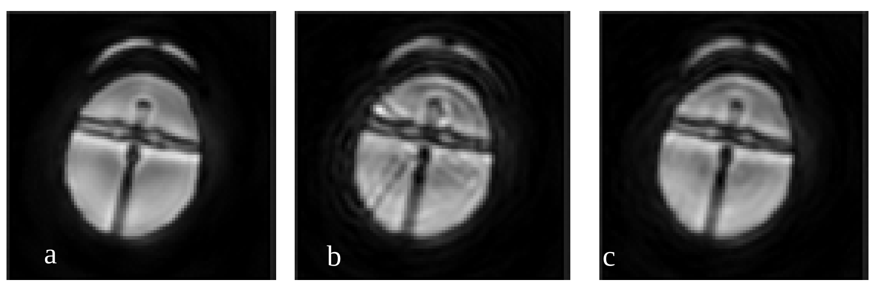

Fig. 2 Axial images of a skull phantom acquired using the shells trajectory both without (a) and with (b) motion. The corresponding image after motion correction are shown in (c). Only the central 18×18 cm^2 FOV is shown here.

Phantom experiment: A gel-filled model of a human skull was used to test the motion correction algorithm. Three inductively-coupled point markers [6] filled with copper sulfate solution were affixed to the phantom. A reference data set was collected using the shell trajectory by keeping the phantom stationary. In the second scan, the phantom was manually rotated in the 45% of the way through the acquisition by approximately 20 degrees. Figure 2 shows images before b) and after c) the motion correction, as compared with the image without motion a). It can be observed that the method can effectively remove the artifacts caused by motion.

Conclusions:

A 3D self-navigated spherical shell trajectory has been described. Without additional data sampling, the k-space obtained with this trajectory can track the 3D rigid body motion of the imaging object accurately. Combined with off-line retrospective motion correction, the trajectory could be used for reduce motion artifacts in a variety of 3D imaging scenarios.

References:

[1] Bernstein MA, Shu Y, Elliott AM, Magn Reson Med 50:802-12, 2003.
[2] Irarrazabal P, Nishimura DG, Magn Reson Med 33:656-62, 1995.
[3] Wong ST, Roos MS, Magn Reson Med 32:778-784, 1994.
[4] Welch EB, Manduca A, Grimm RC, Ward HA, Jack CR Jr., Magn Reson Med 47: 32-41, 2002.
[5] Jackson JI, Meyer CH, Nishimura DG, Macovski A, IEEE: Trans on Med. Imag. 10 (3): 473-478, 1991.
[6] Elliott, AM, Shu Y, Bernstein MA, ISMRM 2432, 2003.